

Report of the Multi-coil Magnetic Field for a Constant Tune Cyclotron

H. W. Koay

TRIUMF

Abstract: This work reports the provisional configuration of a multi-coil setup for a constant-tune cyclotron.

1 Introduction

1.1 Multi-coil Magnetic System

Since the first invention of a cyclotron by Lawrence in 1936, it went through several stages of improvements in the past century in order to improve the versatility of the machine. Advancement in superconducting technology, computing power, as well as the emergence of machine learning and AI technology result in the possibility of having control over a network of multi-coil configuration to accommodate any kind of magnetic field distribution for any type of particle acceleration. Therefore, this work proposes a multi-coil cyclotron design that made up of multiple air-core superconducting coils, aligning side-by-side to each other. The concept of this multiple-coil system is similar to the concept of pixelation, with each pixel is replaced by the a coil. Air-core coils are adopted because the linear dependence between the coil current and magnetic field provides a more direct and simpler optimization [1].

1.2 Constant Tune Cyclotron

A cyclotron has a limited usage when it comes to accelerating particles over a broad energy range. Besides being bounded by its physical size and the limiting axial focusing power at higher energy, the crossing of multiple hazardous resonances are among the most critical issues that limits its application for a wide energy range. In accordance with this, a special type of cyclotron, namely a Constant Tune Cyclotron (CTC), was proposed [2]. CTC that has its tune to remain unchanged from injection until extraction. This causes the resonances-crossing issue to vanish explicitly, and further making it applicable to cover a wider energy range. However, this special type of cyclotron has a rather complex magnetic field distribution in order to support the non-circular orbit of particles. Such a complex B distribution is difficult to be supported by a simple circular coil and spiral edges. Therefore, the multi-coil configuration proposed in this work is a perfect candidate to fit the complex B map of CTC.

2 Basic Specifications

The basic specification of the constant tune cyclotron is given in Table 1. The corresponding magnetic field and its harmonic components needed to keep the tune unchanged are also shown in Figure 1.

Item	Value
Particle type	H ⁺
Energy Range	800 MeV up to 2 GeV
Ave. magnetic field	0.1 ~ 0.55 T
Rev. frequency	~1.97 MHz
Sector number, N	10
Average orbital inner radius (m)	~ 22
Average orbital outer radius (m)	~ 27

Table 1: Basic specification of the constant-tune cyclotron.

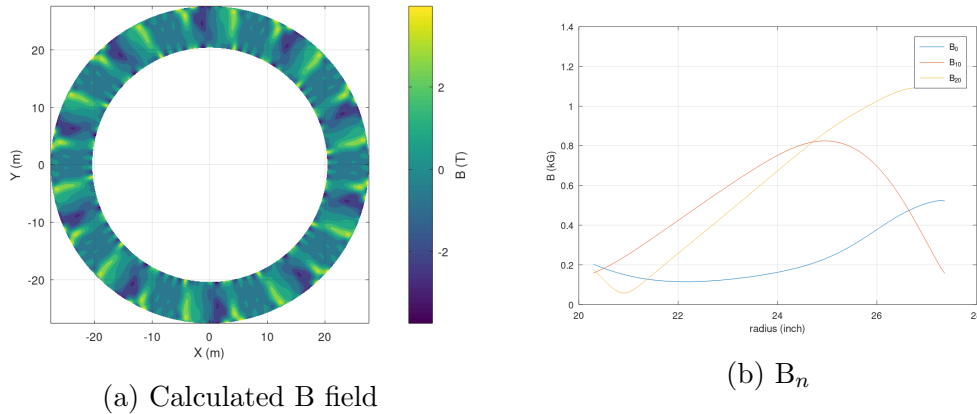


Figure 1: The calculated magnetic field for a constant tune acceleration from 800 MeV up to 2 GeV. (a) shows the 2D distribution at median plan, while (b) shows the n^{th} harmonic of the most prominent terms for this 10-sector cyclotron.

2.1 Coils Configuration

This following will focus only on the discussion of one sector, as similar procedure can be easily repeated for other sectors. Air-core race track coil with the following dimension are arrange side-by-side from an inner radius.

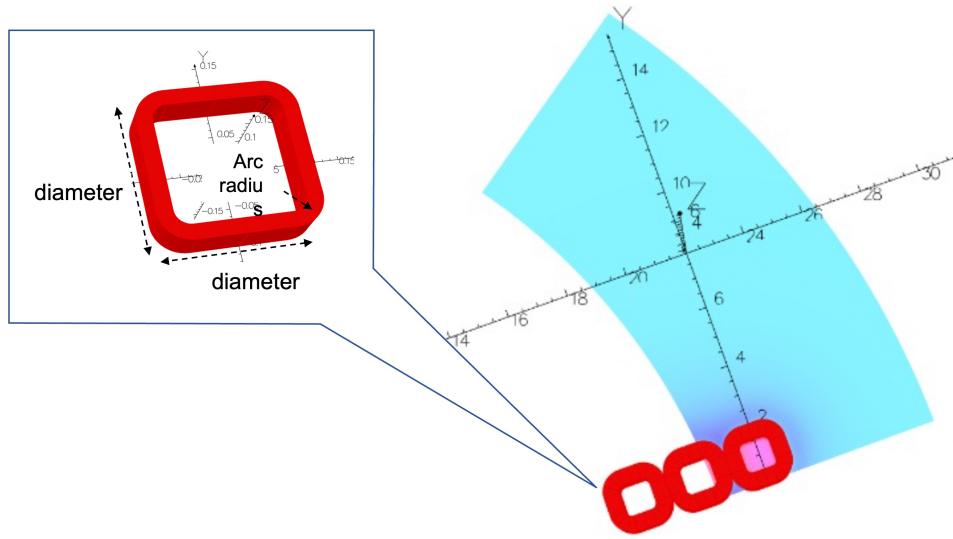


Figure 2: Sample drawing of race-track coils arranging side-by-side to each other for maximum fit.

Item	Value
No. of coils (one sector)	2984
Diameter	20 cm
Cross section (T×W)	$0.2 \times 0.02 \text{ m}^2$
Current density	up to $\pm 1000 \text{ A/mm}^2$
Distance from $z=0$	40 cm
Arc radius	2 cm

Table 2: Configuration of the superconducting coils for the constant-tune cyclotron.

3 Methodology

3.1 Mathematical Formulation of Least Square Method

Owing to the linear dependence between the coil currents and magnetic field, the Least-square method (LSM) can be conveniently used to generate the scaling factor needed optimize B field for constant tune acceleration.

Assuming the axial magnetic field of an n -sectored cyclotron is given by a combination of N trim coils (TC). The B_z at a given radius r and angular position θ is given as eqn. 1. Note that the following discussion drops the

subscript “z” for convenient.

$$B(r, \theta) = \sum_i^N a_i B_{TC,i}(r, \theta) \quad (1)$$

The deviation between B and the ideal field B_{ideal} is

$$\begin{aligned} d_r &= [B_{ideal} - B]_{r,\theta} \\ &= \left[B_{ideal} - \sum_i^N a_i B_{TC,i} \right]_{r,\theta} \end{aligned}$$

The sum-of-square of the deviation of the 2D magnetic distribution up to radius R and angle $\frac{2\pi}{n}$ is given by

$$\begin{aligned} d_{total}^2 &= \sum_r^R \sum_\theta^{2\pi/n} d_{r,\theta}^2 \\ &= \sum_r^R \sum_\theta^{2\pi/n} \left[B_{ideal} - \sum_i^N a_i B_{TC,i} \right]_{r,\theta}^2 \end{aligned}$$

Besides, in order to suppress the tendency of generating huge magnitude of currents with alternative signs from one coil to the next, another term minimizing the total square of current should be included [3].

$$d_{total}^2 = \sum_r^R \sum_\theta^{2\pi/n} d_{r,\theta}^2 + K \sum_i^N a_i^2 \quad (2)$$

The K in equation 2 is a factor that controls the balance between the goodness of fit and the “alternating” behaviour of coil currents. When K is large, the RMS of currents reduces but the field error increases. On the other hand, when K is small, the field error is smaller but the “alternating” behaviour is more significant. This is consistent with our expectation that if $K = 0$, the alternating coil currents are huge.

In order to obtain the smallest d_{total}^2 , partial differentiation of d_{total}^2 over

the adjustable coefficient a_k should be zero:

$$\begin{aligned} \frac{\partial(d_{total}^2)}{\partial a_k} &= \sum_r \sum_{\theta}^{R \ 2\pi/n} -2B_{TC,kr} \left[B_{ideal} - \sum_i^N a_i B_{TC,i} \right]_{r,\theta} + 2K a_k \\ \frac{\partial(d_{total}^2)}{\partial a_k} = 0 &= \sum_r \sum_{\theta}^{R \ 2\pi/n} B_{TC,kr} \left[- \sum_i^N a_i B_{TC,i} \right]_{r,\theta} - K a_k \\ 0 &= \sum_r \sum_{\theta}^{R \ 2\pi/n} \left[B_{TC,k} B_{ideal} - B_{TC,k} \sum_i^N a_i B_{TC,i} \right]_{r,\theta} - K a_k \\ \therefore \sum_r \sum_{\theta}^{R \ 2\pi/n} [B_{TC,k} B_{ideal}]_{r,\theta} &= \sum_r \sum_{\theta}^{R \ 2\pi/n} \left[B_{TC,k} \sum_i^N a_i B_{TC,i} \right]_{r,\theta} + K a_k \end{aligned}$$

Rewrite the whole formalism in matrix form:

$$\begin{aligned} &\begin{pmatrix} \sum_r \sum_{\theta}^{R \ 2\pi/n} B_{TC,1} B_{TC,1} + K & \cdots & \sum_r \sum_{\theta}^{R \ 2\pi/n} B_{TC,1} B_{TC,N} \\ \sum_r \sum_{\theta}^{R \ 2\pi/n} B_{TC,2} B_{TC,1} & \cdots & \sum_r \sum_{\theta}^{R \ 2\pi/n} B_{TC,2} B_{TC,N} \\ \vdots & \ddots & \vdots \\ \sum_r \sum_{\theta}^{R \ 2\pi/n} B_{TC,N} B_{TC,1} & \cdots & \sum_r \sum_{\theta}^{R \ 2\pi/n} B_{TC,N} B_{TC,N} + K \end{pmatrix} \begin{pmatrix} a_1 \\ a_2 \\ \vdots \\ a_N \end{pmatrix} \\ &= \begin{pmatrix} \sum_r \sum_{\theta}^{R \ 2\pi/n} B_{TC,1} B_{ideal} \\ \sum_r \sum_{\theta}^{R \ 2\pi/n} B_{TC,2} B_{ideal} \\ \vdots \\ \sum_r \sum_{\theta}^{R \ 2\pi/n} B_{TC,N} B_{ideal} \end{pmatrix} \end{aligned}$$

It can be represented by

$$\mathbf{M} \cdot \mathbf{A} = \mathbf{B} \quad (3)$$

$$\text{where } \mathbf{M}_{ik} = \sum_r^R \sum_{2\pi/n} B_{TC,i} B_{TC,k} + K \cdot I \quad (4)$$

$$\mathbf{A}_i = a_i$$

$$\mathbf{B}_i = \sum_r^R \sum_{2\pi/n} B_{TC,i} B_{ideal}$$

Solving 3 by gaussian elimination, we can solve for A_i . a_i is the scaling factor of each TC, i.e. by adjusting the current of the TC in accordance to a_i , we can determine the most optimized condition producing the least deviation from the ideal field at a given configuration.

3.2 Dependence of Parameters

The coil diameter (d) and the distance to median plane (g) play important roles in achieving sufficient fitness of the unique B map. The dependence of these parameters were also investigated. The total discrepancy between the fitted and the desired map are given as $\Delta B = \sqrt{d_{total}^2}$, while the standard deviation of the coil current density is given as σ_J . Besides, the K-parameter introduced in eqn. 2 also affects the ΔB and σ_J . The effect of K is also given in Fig. 3.

Diameter, d (cm)	20	20	20	40	60
Distance to median plane, g (cm)	20	30	40	40	40
ΔB (T)	3.7	2.6	2.2	4.2	9.6
σ_J (mA/mm ²)	326	267	422.7	399.4	529.7

Table 3: Dependence of parameters. All the K were set to be 1×10^{-5} .

From Table 3, ΔB increases with increasing d and decreasing g. Therefore, after considering both factors, d=20 cm and g=40 cm were chosen. On the other hand, generally, when the K-value is large, σ_J is low, but ΔB is large. However, when $K < 1 \times 10^{-6}$, lowering K led to “overfit” and worsens the

ΔB . Therefore, a suitable K value of not less than 1×10^{-6} was used. The results of this configuration will be discussed in the next section.

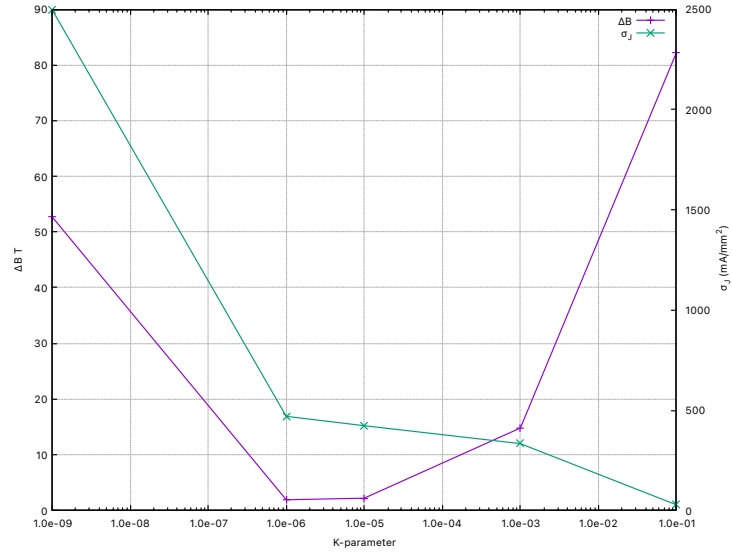


Figure 3: The effect of K-parameter on ΔB and σ_J

4 Results and Discussions

4.1 Magnetic Field Distribution

After optimization, the fitted magnetic field with the current density distribution are shown in Figure 4. The field error, i.e. difference between the fitted field and the desired field is shown in Fig. 5.

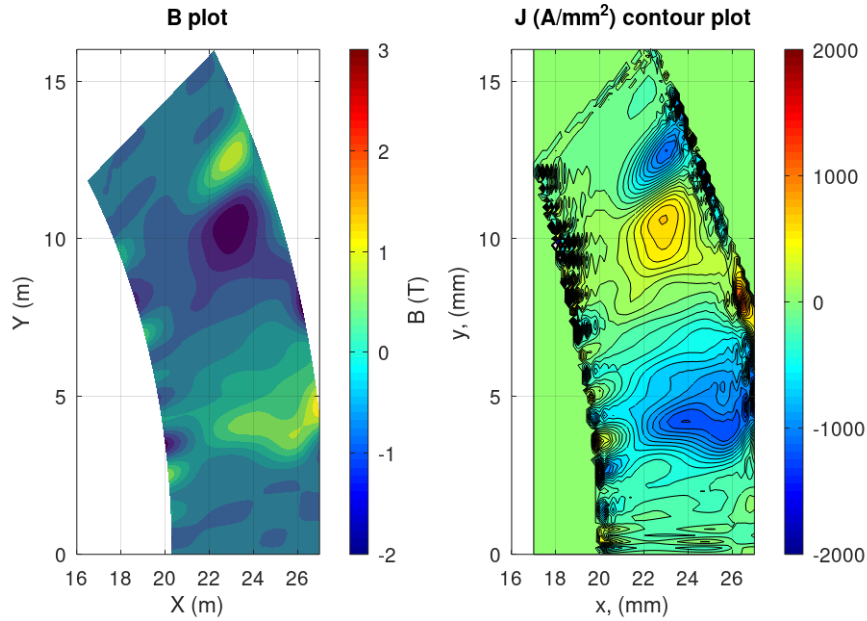


Figure 4: Fitted (left) magnetic field distribution and the contour plot of the current density.

4.2 Tune

The corresponding tune and frequency error are also given in Figure 6. The tunes fit the desired values well with minimal fluctuation. The frequency error is slightly off setted but the deviation remains satisfactory ($< 0.0001\%$). The corresponding tune diagram is also given in Fig. 7. The blue line in the tune diagram shows no crossing to any nearby resonance. This shows a satisfactory performance from the multi-coil B proposed in this work.

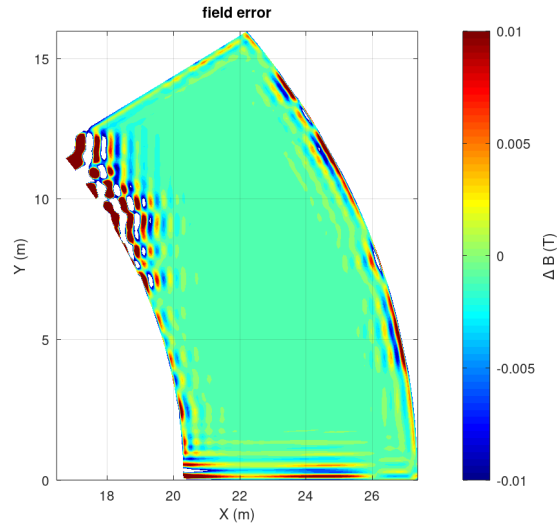


Figure 5: The difference between the desired and the achieved magnetic field at the mid-plane.

5 Summary and Prospects

As a conclusion, this work proves the feasibility of customizing the multi-coil configuration for a complex magnetic field from CTC. This air-core multi-coil configuration has an advantage of being versatile to be applied onto any kind of magnetic distribution. However, the realistic practicality remains a great concern. For instance, more than ten thousands coils are needed to build a full cyclotron like the one shown in this work, with each of them running a different current. This is a challenging task. More works shall be done to look into improving the structure, or maybe to shape several bigger trim coils, with some smaller trim rings around them to tune the match. This shall remain as the next phase of this work.

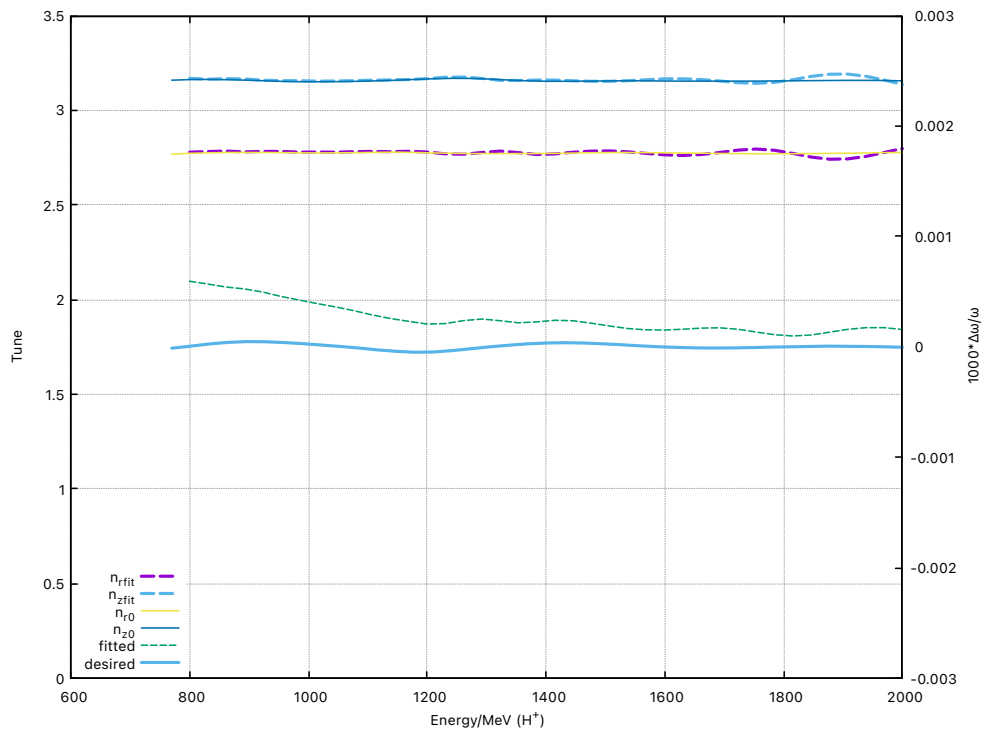


Figure 6: ν_r , ν_z and frequency error ($\times 1000$) for the fitted and calculated B distribution. The desired ν values are shown in solid lines, while ν from fitted B map are shown in dashed lines.

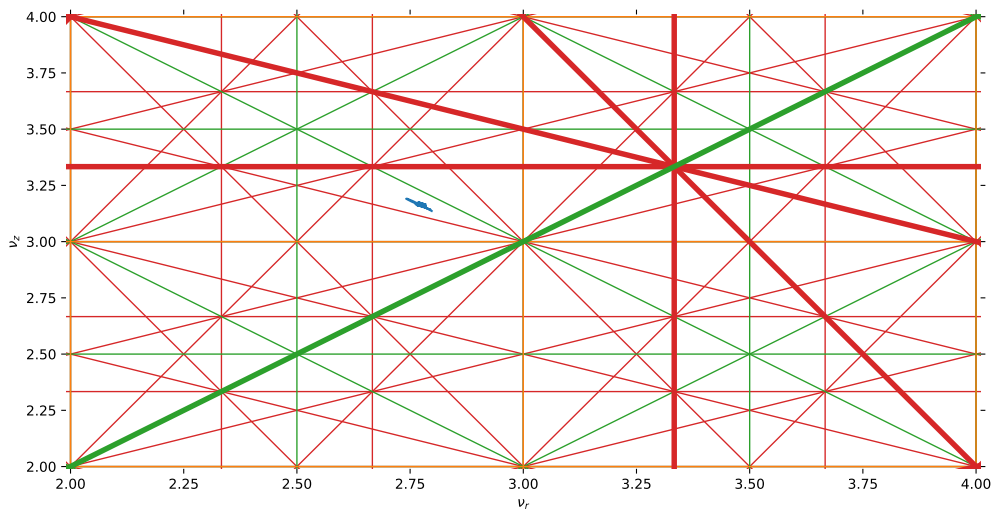


Figure 7: Tune diagram of the fitted B distribution.

References

- [1] H.W. Koay et al. “Beam dynamics and characterization of a new high-intensity compact air-core high temperature superconducting skeleton cyclotron (HTS-SC)”. In: *Results in Physics* 33 (2022), p. 105090. ISSN: 2211-3797. DOI: <https://doi.org/10.1016/j.rinp.2021.105090>. URL: <https://www.sciencedirect.com/science/article/pii/S2211379721010676>.
- [2] Thomas Planche. “Designing Cyclotrons and Fixed Field Accelerators From Their Orbits”. In: *22nd International Conference on Cyclotrons and their Applications (CYC2019)*. 2020, FRB01. DOI: [10.18429/JACoW-Cyclotrons2019-FRB01](https://doi.org/10.18429/JACoW-Cyclotrons2019-FRB01).
- [3] J. Rivers Moore. *Trimfit - Least Squares Fitting Program for Trim Coils*. Tech. rep. TRIUMF, 1970.